



https://doi.org/10.30678/fjt.99931

© 2021 The Authors

Open access (CC BY 4.0)

Study On Effect of Boron Carbide, Aluminium Oxide and Graphite On Dry Sliding Wear Behaviour of Aluminium Based Metal Matrix Composite at Different Temperature

Sharath B N, C V Venkatesh

Department of Mechanical Engineering, Malnad College of Engineering, Hassan, VTU, Belagavi, Karnataka, India

Corresponding author: Sharath B N (sbn@mcehassan.ac.in)

ABSTRACT

The present research has been conducted to study the impact of boron carbide (B_4C), aluminium oxide (Al_2O_3) and graphite on Aluminium 2219 (Al_{2219}). According to current research, B_4C and graphite material be a good substitute for Al_{2219} . Reinforced composites and unreinforced Al_{2219} prepared by a stir casting process. A scanning electron microscope was used to analyze the reinforcement and distribution in the matrix and worn surface of the specimen. Exceptional wear resistance (30%) exhibited by B_4C and graphite-reinforced hybrid composite at 150 °C in contrast with the unreinforced Al_{2219} . The B_4C and Gr reinforcement particulate existence improves the strengthening kinetics in the matrix phase at 150 °C. The artificial neural network used to get the test significance, normalized factor importance and absolute relative error of less than 1%.

Keywords: Artificial neural network, oxide layer, worn surface, metal matrix composites

1. Introduction

The virtue of enlightenment which we enjoy today, is essential due to the improved quality products obtained. Enhancement in the quality of goods can be achieved by a genuine design that considers the functional requirement and its manufacturing aspects. The design process should take proper care of the synthesis technique, which should be an ideal one ensuring the better product is being made available at an economical cost [1]. Furthermore, the productive manufacturing process is an imperative consideration to be accessible in modern industries. Also, the produced product has to competitively priced and should be functional concerning the environment and aesthetic appeal [2]. Aluminium (Al) alloys are of great importance for the transportation sector because of their high strength-to-mass ratios. Still, adhesion is a typical hindrance in the forming and machining of these alloys [3]. AMMCs (Aluminium metal matrix composites) are better at replacing traditional aluminium alloy because of their characteristics [4]. AMMCs exhibit higher wear resistance than monolithic materials [5]. Ceramic reinforced composites are rapidly developing fields due to their progress in the aerospace, aircraft and automobile industries. The lower specific gravity of these materials makes their properties superior concerning mechanical and physical properties [6]. The intensive study into the fundamental properties of the composite materials by reinforcing ceramics to understand their nature, structural and physical properties. To obtain better properties of the material, constituting phases must be altered [7]. The inclusion of small quantities of strong hard

particles significantly increased stiffness, creep and wear resistance [8, 9]. It is now well recognized that ceramic reinforcement dispersion in AMMCs contribute to substantial increases in rigidity and wear resistance [10]. There was a limit above which the addition of graphite (Gr) or SiC (Silicon carbide) was not favourable for the Al-Gr/Al-SiC composite [11]. Incorporating graphite as primary compliance improves the composites wear-resistance by creating a protective layer between the pin and the counter side and exceptionally influences wear resistance by adding alumina as secondary compliance [12]. Better hardness is exhibited when Al alloy reinforced with Al_2O_3 [13]. Many studies have concentrated on the manufacture of SiC, Al_2O_3

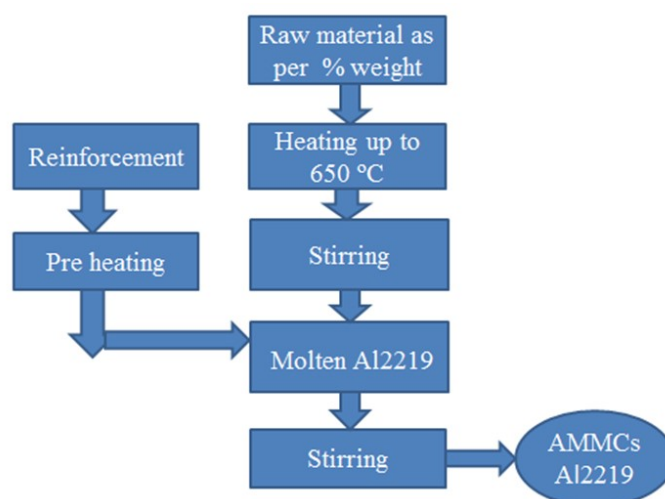


Figure.1: Methodology adopted for AMMCs casting.

Table 1: Materials used for the synthesis of composite

Materials Used for the synthesis of composite
Aluminium 2219
Magnesium as wettability agent
Boron carbide (B ₄ C)
Graphite
Aluminum oxide(Al ₂ O ₃)
Hexa-chloroethane to remove gas from the molten metal

(aluminium oxide) and TiB₂ (Titanium diboride) as refinement material. But there is limited use of the B₄C particles [14]. Silicon (Si) was the well known alloying material found in most aluminium casting alloys. Three main types of Al-Si alloy systems are Hypereutectic (14-25 wt % Si), Eutectic (12-13 wt % Si), Hypoeutectic (<12 wt % Si) [15]. To maximize the engine block's efficiency, Cu (copper) and Mg (magnesium) were added into Al alloys that work at a wide variety of temperatures and stresses [16]. Cu (0.2-2.5 wt %) influences the strength and hardness of aluminium alloy at room and elevated temperature [17]. To avoid clustering of graphite particles, Mg was added into the matrix; thus, the physical and mechanical properties of the aluminium matrix enhanced [18, 19]. The Artificial Neural Network (ANN) was an iterative technique that would be the most popular algorithm to several metallurgy investigators [33]. This is a statistical method used to solve various technical and research problems [34,35].

Literature shows relatively little details on advances in the 2XXX aluminium alloy series reinforced with boron carbide-graphite, Al₂O₃-graphite particles, and very little data is available on dry sliding wear properties at high temperature. Keeping in view of the literature survey, current work was aimed at developing new hybrid composites. Therefore this study attempted to investigate the high-temperature dry sliding wear behaviour of new (Al - 0.02 % Mg - 0.2% Si - 6.8% Cu - 0.25% Zr) heat resistant aluminium alloy 2219 and strengthened by ceramic particulates Al₂O₃, B₄C and graphite. New AMMCs was manufactured by using a stir casting process.

2. Experimental procedure

2.1 Materials and Synthesis of Composite

The stir casting route has done the solidification process. The methodology adopted for AMMCs casting, as shown in figure.1 and the material used to synthesis AMMCs, are listed in table 1, weighed commercially available Al2219 was melted at 650 °C in a pottery-graphite crucible, meanwhile the magnesium lump of 3 wt. % added to the same for further enhancement of wettability.

Table 2: Constituents of Al2219 [21]

Constituents	Si	Mg	Zr	Cu	Fe	Mn	Ti	V	Zn
Weight %	0.2	0.02	0.1-0.25	5.8-6.8	0.3	0.02	0.02	0.05	0.1

Table 3. Material composition in percentage [15]

Sample	Al2219	B4C		Al2O3		Graphite, wt. %
		wt. %	wt. %	wt. %	wt. %	
A	100	-	-	-	-	-
A1	90	-	5	-	-	5
A2	90	5	-	-	-	5

Once the collected ingot in the crucible reaches a liquid state over time, a certain slag was collected at the top and removed to avoid casting defects. After that, preheated commercially available weighed Al₂O₃ (30µm) was added as reinforcement into the crucible. The desired times of the elapsed stirring (speed of 150 rpm) occur in the crucible to give a proper homogeneous mixture. Preheated graphite was added into the crucible as a secondary reinforcement, and the same procedure was adopted to get a hybrid homogeneous mixture [20]. The mixed molten metal slurry is poured into a split type preheated permanent graphite mould. The hybrid composites have been synthesized by reinforcing wt.% of Al₂O₃, graphite, B₄C powder (30µm). Constituents of Al2219 is shown in table 2.

2.2 Microstructure and XRD

The Microstructure and worn surfaces of the tests specimens were studied using a scanning electron microscope (SEM) (high-performance Quanta 200 FEG-SEM) magnification range:12x to 1,00,000. Backscatter Diffraction was used to capture the image. Captured SEM images help to see the microstructure and worn surface of the test specimens. The diffractometer equipped with CuK radiation k₁:54 _ AP. During XRD examination, an angle of 10-80 ° for the diffraction angle (2θ) was maintained [24].

2.3 Hardness test

The hardness of a specimen was measured (Model: PHB-3000) by pressing chromium-steel or tungsten-carbide against the surface of a test specimen. Samples were prepared as per ASTM E-10 standards (IS 1500 (II): 2013, ISO

Table 4. Factors and their levels used in the study.

Factors	Levels		
	1	2	3
Load, N	20	30	40
Speed, m/s	1.25	2.5	3.75
Sliding distance, m	400	600	800
Temperature, °C	50	100	150

Table 5. Layout plan and experimental results.

Exp. runs	Load (N)	Speed (m/s)	Distance (m)	Ttemperature (°C)	Wear rate mm/m ³		
					Sample A2	Sample A1	Sample A
1	20	1.25	400	50	0.9247	1.0471	1.1734
2	20	1.25	600	100	0.5724	0.6437	0.7356
3	20	1.25	800	150	0.2807	0.3754	0.4376
4	20	2.51	400	100	1.0898	1.13456	1.2045
5	20	2.51	600	150	0.9467	1.0567	1.1435
6	20	2.51	800	50	1.1063	1.2560	1.3436
7	20	3.76	400	150	0.9347	1.1397	1.2876
8	20	3.76	600	50	1.343	1.4945	1.5478
9	20	3.76	800	100	1.1393	1.2675	1.3956
10	30	1.25	400	100	1.0127	1.1731	1.2674
11	30	1.25	600	150	0.77058	0.9675	1.0345
12	30	1.25	800	50	1.0401	1.1413	1.2876
13	30	2.51	400	150	1.0568	1.1564	1.2543
14	30	2.51	600	50	1.4971	1.5341	1.6341
15	30	2.51	800	100	1.2634	1.3436	1.4765
16	30	3.76	400	50	1.7833	1.8331	1.9761
17	30	3.76	600	100	1.2549	1.3564	1.4871
18	30	3.76	800	150	1.0726	1.1543	1.2358
19	40	1.25	400	150	1.1889	1.2987	1.3456
20	40	1.25	600	50	1.2989	1.3659	1.4567
21	40	1.25	800	100	1.10634	1.2568	1.3456
22	40	2.51	400	50	1.9154	2.0145	2.1678
23	40	2.51	600	100	1.4321	1.5678	1.6789
24	40	2.51	800	150	1.1286	1.2674	1.3456
25	40	3.76	400	100	1.4318	1.5678	1.6398
26	40	3.76	600	150	1.343	1.4567	1.5768
27	40	3.76	800	50	1.5791	1.6578	1.7658

6506: 2005). The hardness number was reported from digital testers at the load of 240 kgf and dwell time of 30 sec [25].

2.4 Wear test

By conducting wear tests, it helps to discern wear properties. Measurable wear depends on the measuring method. In general, two ways are accessible to measure wear rate, such as weight loss and volume loss, out of which

mass-loss method is the amenable method. In this method, weight loss must not be varied with condensed moisture and other foreign contaminants such as oil, dust etc. On the other hand, volume loss is also the best method to measure wear, but it is a more sensitive method [22]. Pin-on-disc (Pin heating-wear and friction monitor TR-20-PHM 400) testing apparatus was used to discern dry sliding wear behaviour of Al2219 and AMMCs at different temperature. As per the G99 standard [23], 10 mm diameter round pin of the AMMCs were made to slide against the rotating steel

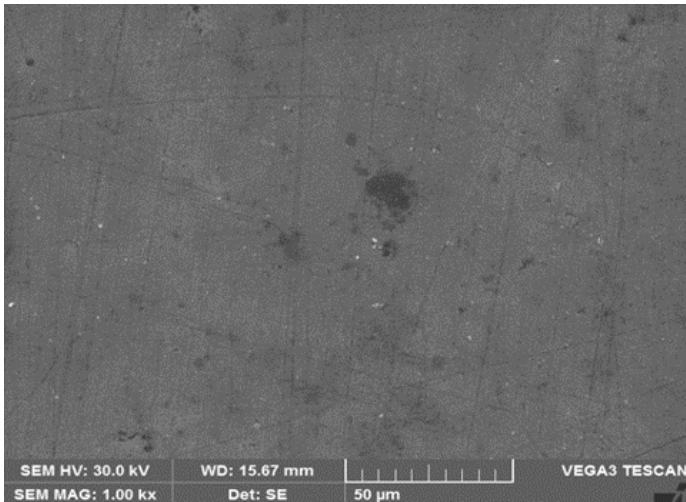


Figure.2: Microstructure of specimen A

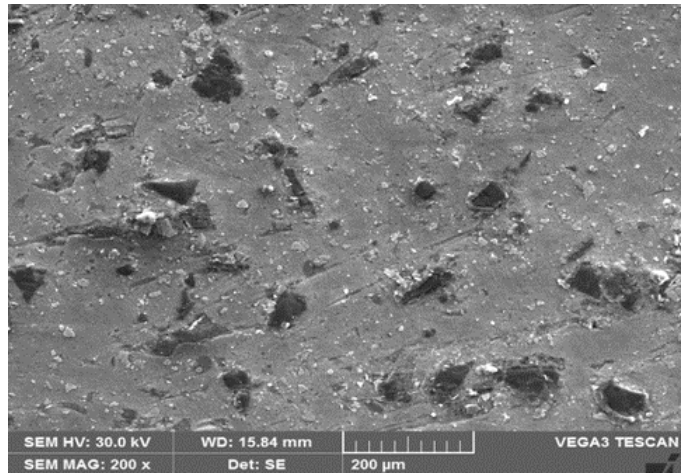


Figure.4: Microstructure of specimen A₂

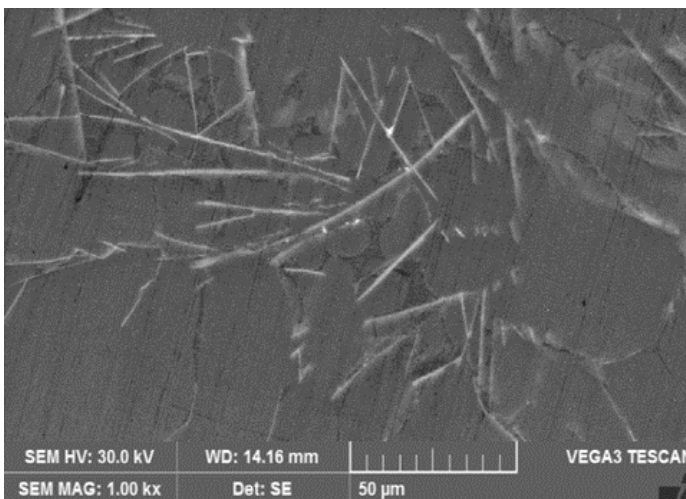


Figure.3: Microstructure of specimen A₁

disc (steel EN - 32) at different temperatures such as 50 °C, 100 °C and 150 °C [21]. While conducting the test, acetone was used to clean the specimen and disc. Here, acetone acts as a chemical agent to protect the surface of the test pin and steel disc from the atmosphere. Before and after, the test specimen's mass was recorded using an Electronic balance weigher (0.0001 g resolution). Table 4 shows wear test parameters.

2.5 Design of Experiments

Taguchi's L27 orthogonal array is used to design the experiments. The experimental layout plan and measured average responses are presented in table 5. Load, Speed, Distance, and temperature are taken as input parameters, whereas wear rate is the responses.

3.Result and discussions

3.1 Microstructural Examination

XRD pattern and SEM of the matrix alloy and hybrid composites for the corresponding composition is shown in

figure (2-7). The results obtained from XRD analysis revealed that the firm peaks belong to the parent material, i.e., aluminium. The smaller peaks also indicate Cu, Mg and B₄C in the hybrid composites(A₂).Al₂O₃ also presents as seen in smaller peak (A₁).

The microstructure of this hybrid composite shown by SEM images Fig.2-4. The bright area indicates oxides and is evident enough to show the discrete particles, and no appreciable accumulation was observed in fig. 3. On the other hands, the intermetallic Al₃Mg₂ seems like a flake shape and are small. A dark spot noticed, and its indicate porosity in the hybrid composite. Fig .4 shows the distribution of B₄C and graphite [similar result observed by Kumar et al. and sing et al.]

3.2 Hardness test

Figure.8 illustrates the hardness values of the test samples. It is confirmed that sample A₂ exhibits higher hardness than A₁ and A. Due to the existence of B₄C and graphite, the hardness of the composites increased. B₄C was the third hardest material, and it acts as a barrier to dislocation; meanwhile, the strengthening effect of graphite also influences the hardness of the composite.

3.3 Wear Analysis at Different Temperatures

Microscope images help visualize the typically worn surface of a pin due to the adhesion of wear debris wear tracks formed [Wang et al. Observed similar result] on the sample, as clearly seen in fig 11. Due to the formation of the oxide transferred layer, the worn surface is enfolded. It minimizes the direct metal to metal contacts between the interface, thereby minimizing weight loss. However, the tribo-layer is not a permanent layer at higher loads; this tribo-layer gets ruptured and tends to increase the wear rate, as shown in fig.11. The microstructure of the new alloy predominantly comprised of Al-Cu-Mg and matrix phase was analyzed and confirmed as an incoherent interface with a matrix that also influences the wear rate [similar result observed by Rajaram et al.]. Comparing worn surfaces of Al₂O₃ reinforced composite, the Al2219

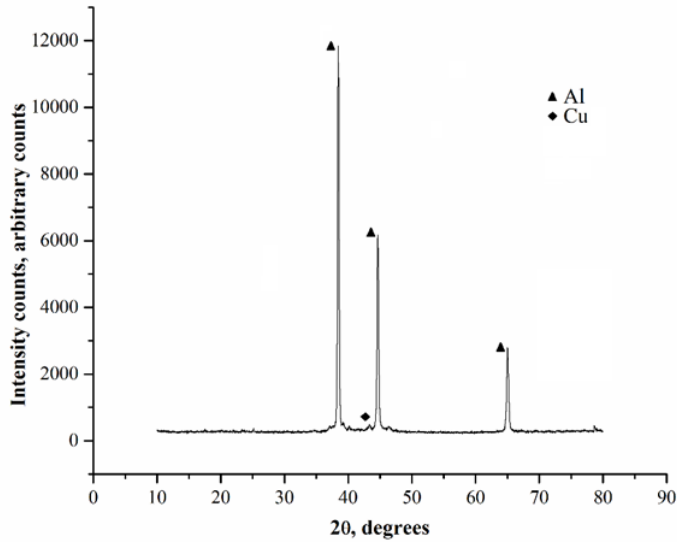


Figure.5: XRD of specimen A

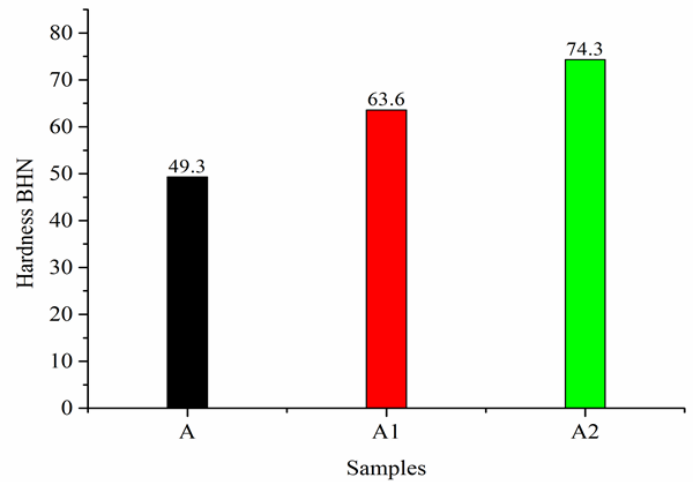


Figure.8: Hardness value

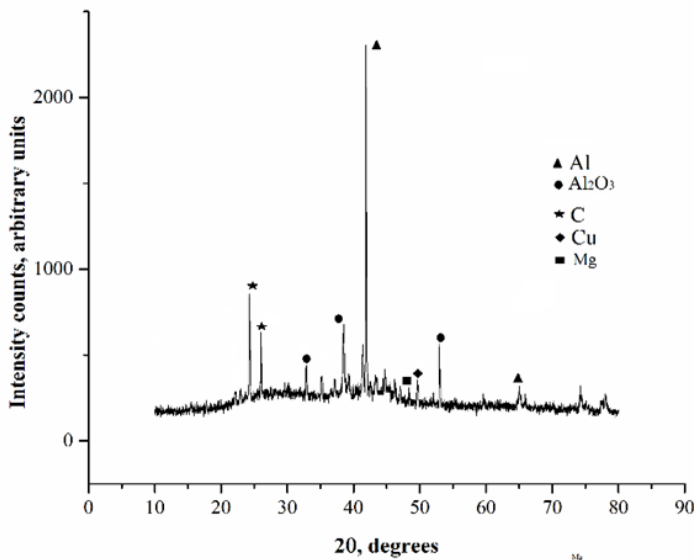


Figure.6: XRD of specimen A₁

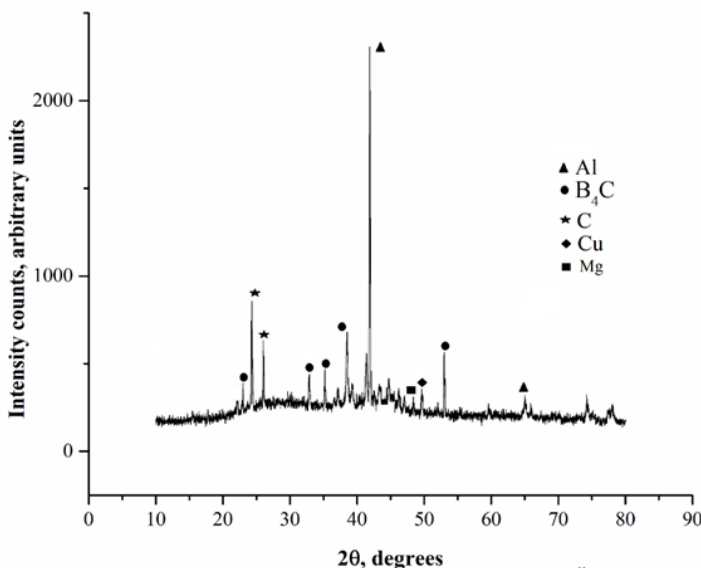


Figure. 7: XRD of specimen A₂

alloy surface became more damaged because of temperature. Due to synergetic action between Al_2O_3 and matrix, it exhibits more excellent wear resistance than unreinforced alloy, as shown in fig.9 [Wang et al. obtained similar observation]. Transition temperature between mild and severe wear not occurred. Thus wear resistance of the composite (A1) decreased monotonically at 150 °C. Such variations can be seen in fig.12 [Mart'in et al. obtained similar observation].

The tests were done varying the normal load. At the atomic level, the surface of a material can not be entirely flat. When two surfaces are in contact, they touch each other at some points. When the load is applied, plastic deformation occurs locally in those points, which leads to the removal of material. More the load more will be the plastic deformation. Hence wear rate will be more at 40 N. Rate of plastic deformation will depend on applied load; therefore, less wear rate occurs at load 20N.

On the other hand, delamination was one of the most popular mechanisms which will drive the wear phenomenon, and the same can be seen from SEM images. When the two interacting surfaces slide against each other under load and heat, it can be observed, which results in the detachment of wear particles in the form of sheets or flakes. Moreover, ploughing action insists on taking plastic deformation and plastic flow at the asperities, as seen in SEM [similar result observed by Suresh et al.].

Graphite is acting as secondary reinforcement. It has a unique molecular structure consisting of a hexagonal carbon sheet held by strong hybridized carbon-carbon bonding; the motion of these sheets is easy to slip over each other, which results in excellent lubricating ability [4]. SEM observation results of the new alloy represented the ductile fracture mode with equi-axied crystals. Equi-axie crystals were mainly initiated by adding reinforcement due to uniform cooling. Due to the effect of B_4C and Graphite, the rate of heat dissipation was reasonable; as a result, uniform crystals were formed.

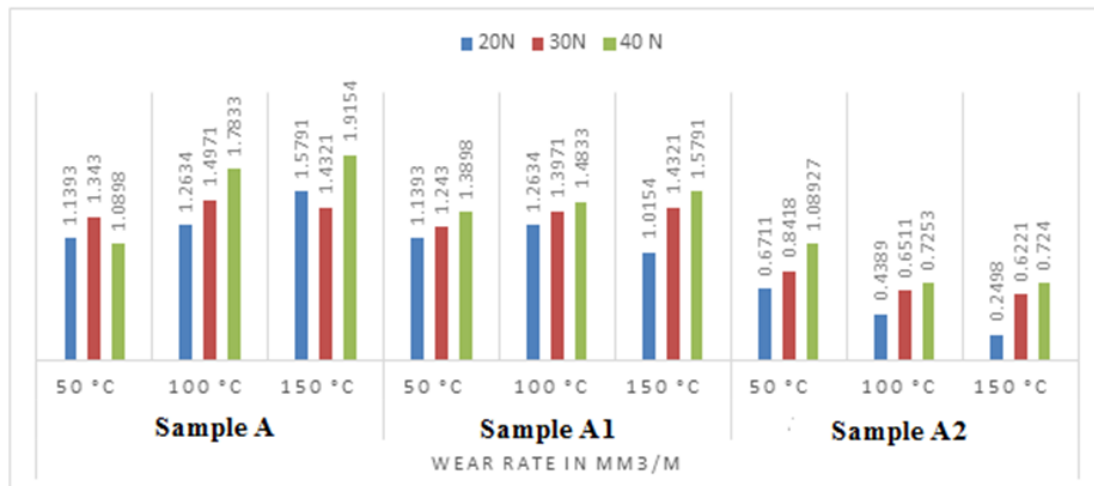


Figure.9 Load vs temperature

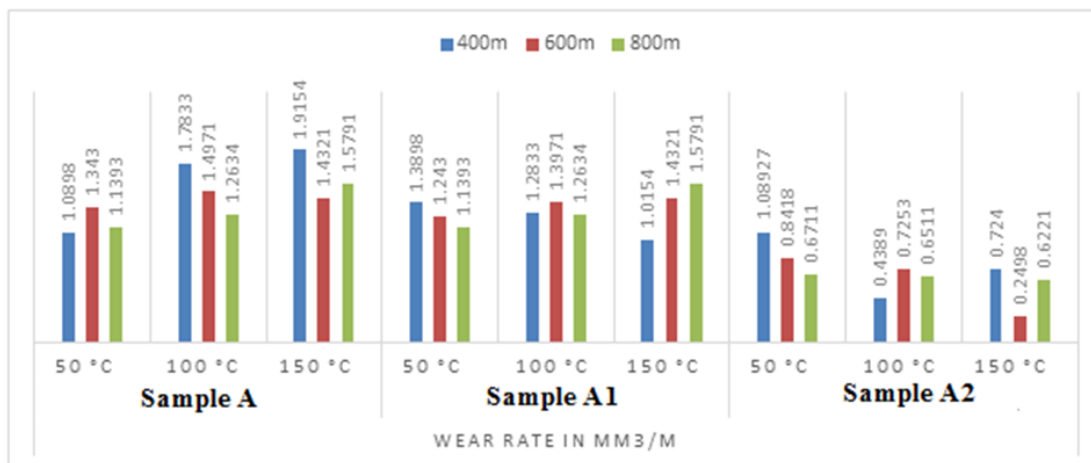


Figure.10 Temperature vs sliding distance

It was interposed that, though the AMMCs temperature was 150 °C still wear resistance of the composite could be maintained by reinforcement. Sample A2 possesses significantly improved wear resistance and hardness (74.3 HN) contributed by the 5 % B₄C and 5 % graphite reinforcement. However, these composites A2 are capable of performing at elevated temperatures substantially higher than A and A1. When B₄C and graphite particulate as added into Al2219 tends to form layers that act as a preservative barrier which leads to creating an obstacle for dislocation. The dispersion-strengthening effect plays a significant role in improving wear resistance. Also, it is sustained at both ambient and high temperatures over prolonged periods [similar result observed by Biswas et al.]. According to current exploration, it clearly says that B₄C and graphite content is an appropriate alternative to the conventional alloy to attain a higher wear resistance at 150 °C. The existence of B₄C and graphite particulate may improve the strengthening kinetics in the Matrix phase.

From the experimental findings (fig. 10) shows that. Wear resistance was improved due to the longer sliding distance. During high-temperature sliding, tearing of oxide

layers occurs because of thermal stresses and compaction due to applied pressure resulting in agglomerated clusters of oxide wear debris. Eventually, due to temperature and applied pressure, sintering of fine wear debris occurs. The rate of sintering increases with the increase in temperature, resulting in solid smooth, hard surfaces, termed as tribo-layer. The tribo layers protect the sliding surfaces for a longer time from developed forces, and hence the wear rate is reduced. The failure of tribo layer leads to the formation of the oxide layer and tearing of the oxide layer, resulting in sintering of the wear debris and the process getting repeated. It is evident from the wear trend that the tribo layer effect was not influenced at room temperature for alloy and composite.

So far, few studies noticed the effect of ceramics on Aluminium. In this contrast, Al2219-B₄C-graphite composites retain their high-temperature strength compared to the unreinforced matrix and Al2219-Al₂O₃-graphite. therefore, the possibility of further enhancement by increasing wt. % of B₄C and graphite particulates, and this segment additions is an attractive one and worth pursuing.

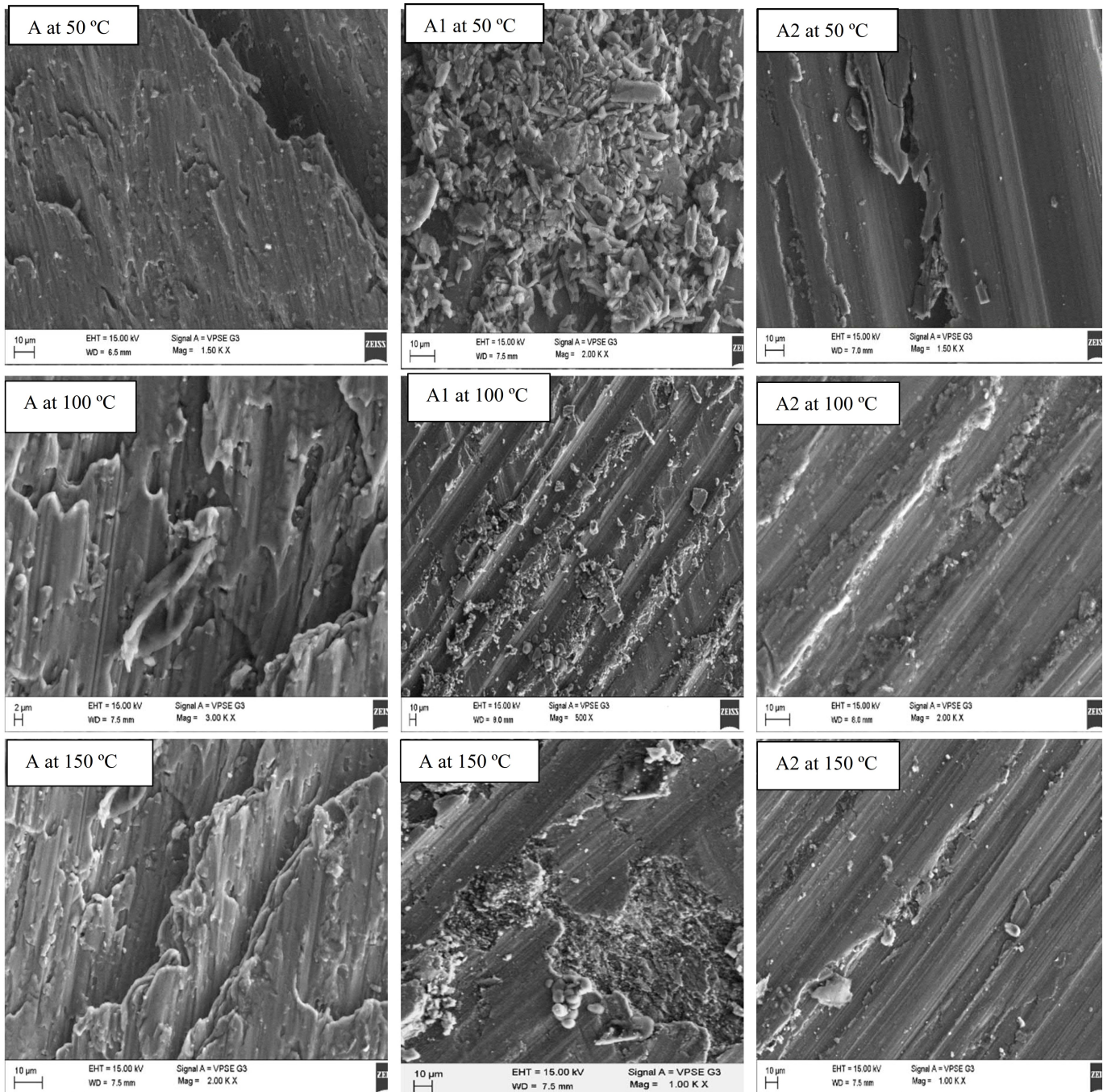


Figure.11 The worn surface of the test Pin at different temperature

3.4 Artificial neural network

IBM SPSS Statistics.22 was used to employ the ANN framework to predict the wear properties of the composite. An artificial neural network is an effective tool used to predict the wear properties of the alloy and AMMCs by the multilayer perceptron method. Five input vectors were used in constructing the proposed network (L: Load, S: Speed, D: Distance, T: Temperature, and W: Wear rate). Satisfactory effects can be calculated using the ANN outputs, thereby minimizing time and expense for research.

3.4.1 ANN analysis for sample A:

ANN was developed and deployed to aid a completely backpropagation neural network for this analysis (IBM SPSS Statistics 22). To activate the hidden layers (grey lines), the hyperbolic tangent function was chosen. The proposed ANN involves 27 trail, and the architecture of ANN is shown in fig.12.

An ANN consists of a large number of nodes (blue colour line) and their connections. Each node represents a specific output function termed an activation function.

The experimental values were correlated with expected ANN values to assess the efficiency of the validating pro-

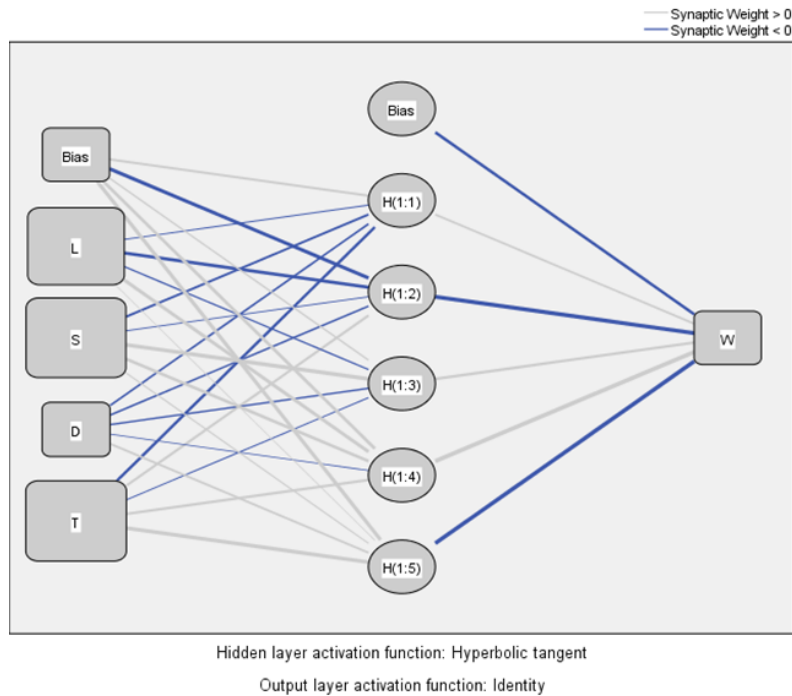


Figure.12 Architecture of ANN

cesses. It can be noted that the predictability of ANN output values significantly closer to experimental values. It is confirmed by seeing error graphs obtained by predicted values and experimental values, as seen in fig. 15. The overall absolute relative error for the estimated value is less than 1 %. Fig.14 confirms that temperature is a more imperative factor to attain maximum wear and followed by load and speed [similar result observed by Hassan et al.].

3.4.2 ANN analysis for sample A1

It is optimal when the ANN input data referred by testing condition. A well-trained ANN is beneficial to estimate the material characteristics. The experimental values were correlated with expected ANN values to assess the efficiency of the validating processes. It can be noted that ANN predictive outcomes fit actual measurement data, as seen in fig. 16. The overall absolute relative error for the estimated value is 0.4%. Fig. 27 is confirmed that load is a more imperative factor to attain maximum wear and followed by speed and temperature.[similar result observed by Zhang et al.]

3.4.3 ANN analysis for sample A2

A well-trained ANN has been used to measure the wear rate based on an experimental dataset for reinforced composites. The obtained result is significantly closer to measured data [Jiang et al. Observed similar result]. Prediction accuracy is also high, as seen in fig. 21. The relative error is 0.2% only and confirms prediction quality as seen in fig.19. Normalized importance of factor is demonstrated load and speed are dominated by attaining higher wear rate in all the samples, as seen in the figure. 20.

4. Conclusions

In the present investigation, Al2219, Al2219+Al₂O₃-graphite and Al2219+B₄C-graphite composites are fabricated using the stir casting technique. Experiments are performed based on the L27 orthogonal array. The following conclusions can be drawn.

- From the SEM analysis, it is concluded that the fabrication of the AMMCs liquid stir casting method is preferred because it yields in proper mixing of reinforcements with parent alloys.
- SEM and XRD confirm the distribution of B₄C and graphite particles in the aluminium matrix.
- Increasing applied load and speed increases wear rate at all the temperature.
- Incorporating B₄C and graphite particles helps the material to resist wear resulting in a lower wear rate.
- Tribo-layer of the AMMCs significantly influenced wear rate. The boron carbide and graphite-reinforced AMMCs (A2) exhibits the lowest wear rate, while Al2219 samples (A) shows the highest wear rate.
- It is also observed that abrasive and adhesive wear is a problem during sliding. This result indicated that B₄C and graphite content is an appropriate alternative to conventional Al2219 metal matrix composites.
- Wear resistance of the hybrid composite A2 is dominant at 150 °C contrast with A1 and A2. Because of

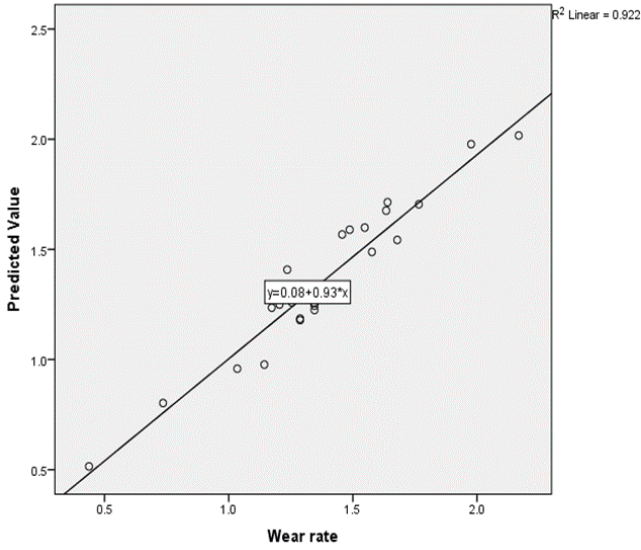


Figure.13 Experimental vs predicted values.

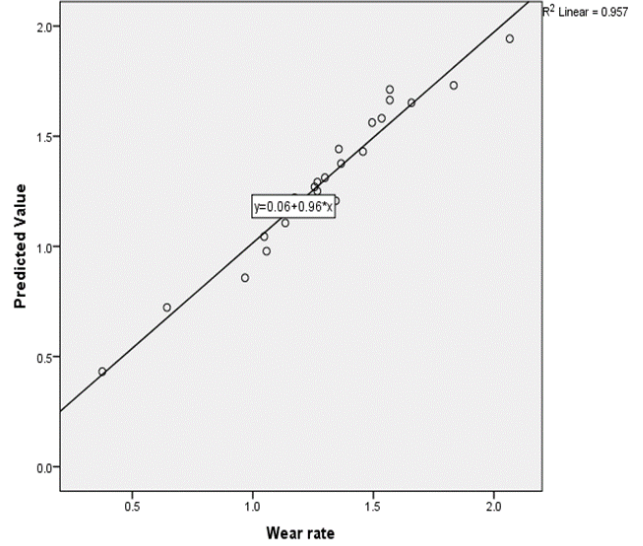


Figure.16: Experimental vs predicted values

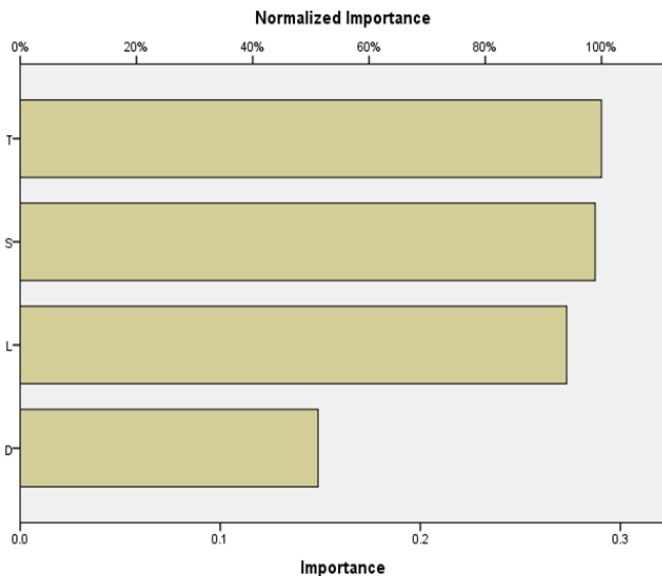


Figure.14 Normalized factor importance

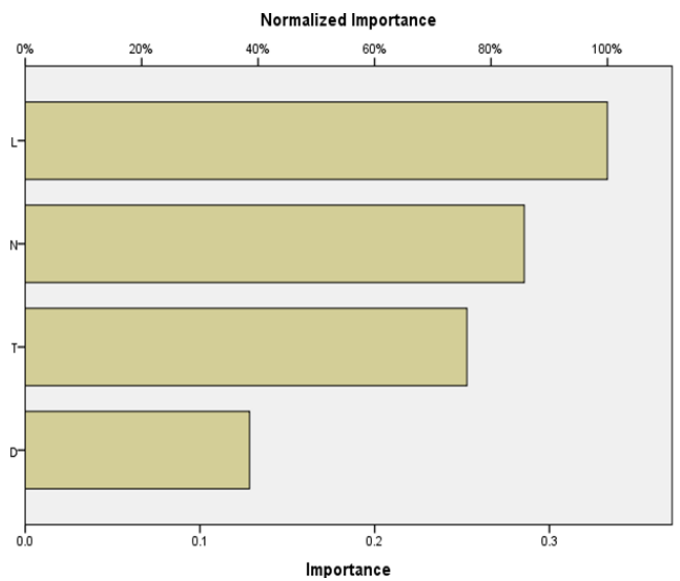


Figure.17: Normalized factor importance

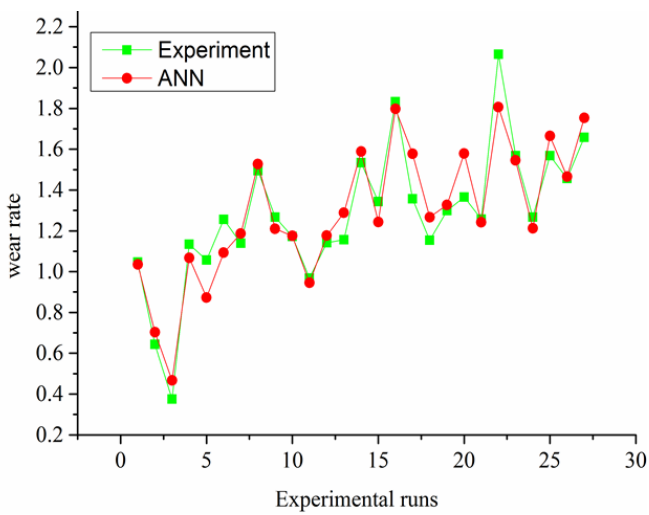


Figure.15 Error values.

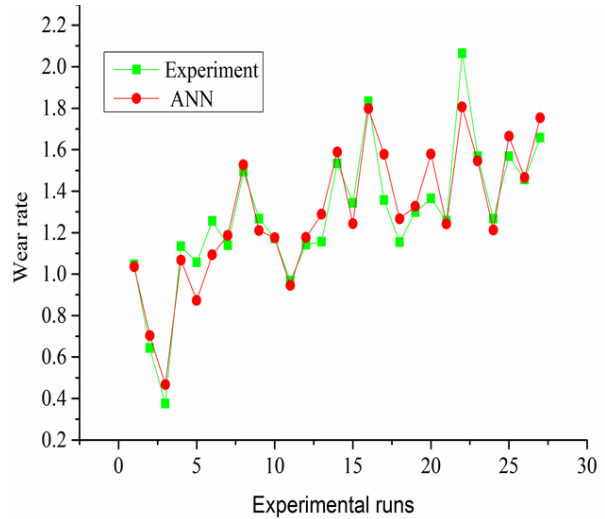


Figure.18: Error values

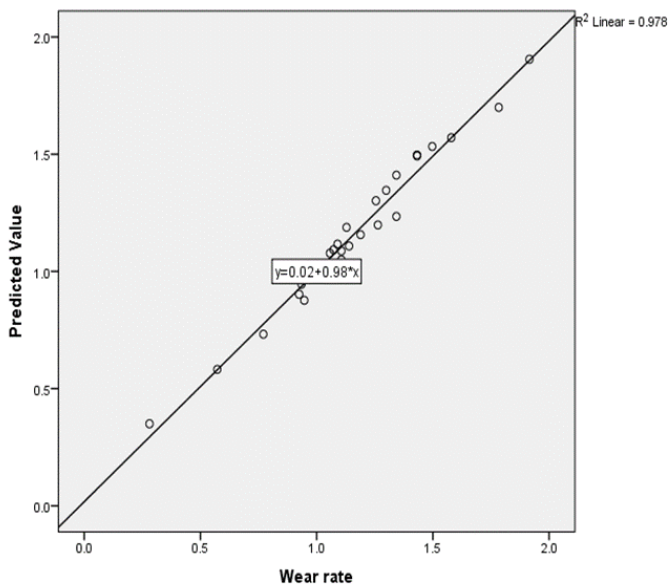


Figure.19 Experimental vs predicted values

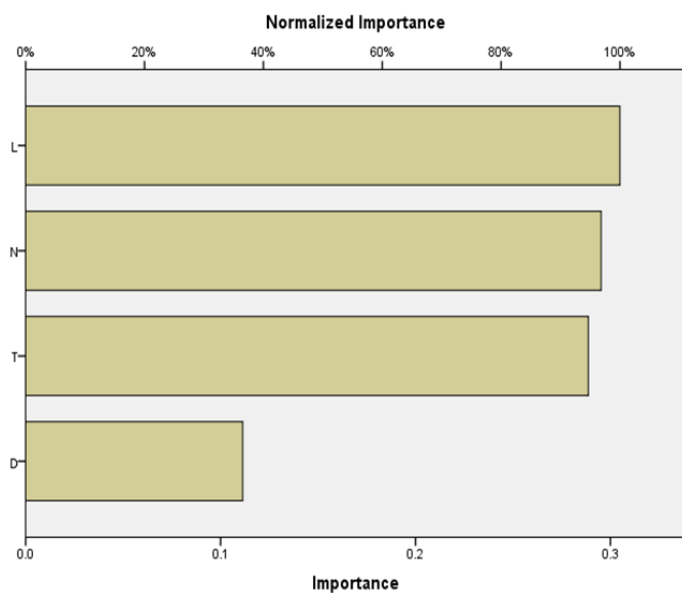


Figure.20 Normalized factor importance

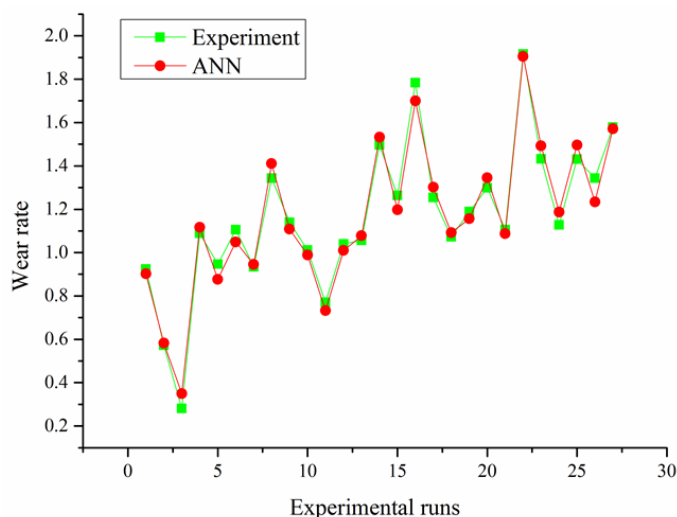


Figure.21 Error values

the solid tribo layer formed by B_4C and graphite, and deterioration rate of tribo layer is meager. Thus boron carbide and graphite-reinforced AMMCs (A2) shows excellent wear resistance at all the temperature.

- ANN is a valuable statistical instrument for analyzing the wear properties of the AMMCs; the relative error predicted values fall within 1 % compared with the experimental results.
- It can be noted that ANN predictive outcomes fit actual measurement data. It is confirmed that load is a more imperative factor to attain maximum wear and followed by speed and temperature.

REFERENCES

- 1 P.R.S. Kumar, S. Kumaran, T. Srinivasa Rao, S. Natarajan "High temperature sliding wear behavior of press-extruded AA6061/fly ash composite", Elsevier -Material Science and Engineering:A, Volume 527, Issue 6, Pages 1501-1509, 2010. <https://doi.org/10.1016/j.msea.2009.10.016>
- 2 Ham, A.L., Yeomans, J.A. and Watts, J.F. Effect of temperature and particle velocity on the erosion of a silicon carbide continuous fibre reinforced calcium aluminosilicate glass-ceramic matrix composite. *Wear*, 233, pp.237-245. 1999 [https://doi.org/10.1016/S0043-1648\(99\)00222-7](https://doi.org/10.1016/S0043-1648(99)00222-7)
- 3.A Abou Gharam,M.J. Lukitsch,,High temperature tribological behaviour of carbon based(B_4C and DLC) coating in sliding contact with aluminum", Elsevier-Thin Solid Films,Volume 519, Issue 5, Pages 1611-1617,30.2010. <https://doi.org/10.1016/j.tsf.2010.07.074>
- 4 Suresha, S. and Sridhara, B.K. Effect of silicon carbide particulates on wear resistance of graphitic aluminium matrix composites. *Materials and Design*, 31(9), pp.4470-4477. 2010 <https://doi.org/10.1016/j.matdes.2010.04.053>
- 5 S.M.R. Mousavi Abarghouie, S.M. Seyed Reihani "Investigation of friction and wear behaviors of 2024 Al and 2024 Al/SiCp Composite at elevated temperatures", Elsevier-Journal of Alloys and compounds,Volume 501, Issue 2, Pages 326-332. 2010. <https://doi.org/10.1016/j.jallcom.2010.04.097>
- 6 Onoro, J., Salvador, M.D. and Cambroner, L.E.G. High-temperature mechanical properties of aluminium alloys reinforced with boron carbide particles. *Materials Science and Engineering: A*, 499(1-2), pp.421-426. 2009. <https://doi.org/10.1016/j.msea.2008.09.013>
- 7 Rana, R.S., Purohit, R. and Das, S. Reviews on the influences of alloying elements on the microstructure and mechanical properties of aluminum alloys and aluminum alloy composites. *International Journal of*

- Scientific and research publications, 2(6), pp.1-7.
2012
8. Gómez-del Río, T., Rico, A., Garrido, M.A., Poza, P. and Rodríguez, J. Temperature and velocity transitions in dry sliding wear of Al-Li/SiC composites. *Wear*, 268 (5-6), pp.700-707. 2010. <https://doi.org/10.1016/j.wear.2009.11.006>
9. A. Martín, J. Rodríguez, J. Llorca "Temperature effects on the wear behaviour of particulate reinforced Al-based composites", Elsevier Volumes 225-229, Part 1, Pages 615-620. 1999. [https://doi.org/10.1016/S0043-1648\(98\)00385-8](https://doi.org/10.1016/S0043-1648(98)00385-8)
- 10 Llorca, J. High temperature fatigue of discontinuously reinforced metal-matrix composites. *International journal of fatigue*, 24(2-4), pp.233-240. 2002. [https://doi.org/10.1016/S0142-1123\(01\)00077-9](https://doi.org/10.1016/S0142-1123(01)00077-9)
- 11 Suresha, S. and Sridhara, B.K. Wear characteristics of hybrid aluminium matrix composites reinforced with graphite and silicon carbide particulates. *Composites Science and Technology*, 70(11), pp.1652-1659. 2010. <https://doi.org/10.1016/j.compscitech.2010.06.013>
12. Radhika, N., Subramanian, R. and Prasat, S.V. Tribological behaviour of aluminium/alumina/graphite hybrid metal matrix composite using Taguchi's techniques. *Journal of Minerals and Materials Characterization and Engineering*, 10(05), p.427. 2010. <https://doi.org/10.4236/jmmce.2011.105032>
- 13 Kumar, A., Lal, S. and Kumar, S. Fabrication and characterization of A359/Al₂O₃ metal matrix composite using electromagnetic stir casting method. *Journal of Materials Research and Technology*, 2(3), pp.250-254. 2013 <https://doi.org/10.1016/j.jmrt.2013.03.015>
- 14 Auradi, V., Rajesh, G.L. and Kori, S.A. Processing of B4C Particulate Reinforced 6061 Aluminum Matrix Composites by melt stirring involving two-step addition. *Procedia Materials Science*, 6, pp.1068-1076. 2014. <https://doi.org/10.1016/j.mspro.2014.07.177>
- 15 Ahmed, A., Wahab, M.S., Raus, A.A., Kamarudin, K., Bakhsh, Q. and Ali, D. Mechanical properties, material and design of the automobile piston: an ample review. *Indian Journal of Science and Technology*, 9 (36). 2016. <https://doi.org/10.17485/ijst/2016/v9i36/102155>
- 16 G. Rajaram, S. Kumaran, T. Srinivasa Rao "High temperature tensile and wear behavior of aluminum silicon alloy", Elsevier Material Science and Engineering: A, Vol 528, issue 1, Pages 247-253, 25 November 2010. <https://doi.org/10.1016/j.msea.2010.09.020>
17. S.G. Shabestari, H. Moemeni Effect of copper and solidification conditions on the microstructure and mechanical properties of Al-Si-Mg alloys *Journal of Materials Processing Technology* 153-154, 193-198. 2004. <https://doi.org/10.1016/j.jmatprotec.2004.04.302>
- 18 Davis, J. R., Corrosion of Aluminum and Aluminum alloys, Ohio, ASM International. 1999. <https://doi.org/10.31399/asm.tb.caaa.9781627082990>
- 19 Mondolfo, L. F., Aluminum alloys: Structure and Properties, London, Butterworths. 1999.
- 20 Gul, F. and Acilar, M. Effect of the reinforcement volume fraction on the dry sliding wear behaviour of Al-10Si/SiCp composites produced by vacuum infiltration technique. *Composites Science and Technology*, 64(13-14), pp.1959-1970. 2004. <https://doi.org/10.1016/j.compscitech.2004.02.013>
- 21 Sharath, B.N., Madhu, K.S. and Venkatesh, C.V. Experimental Study on Dry Sliding Wear Behaviour of Al-B4C-Gr Metal Matrix Composite at Different Temperatures. *J. Applied Mechanics and Materials*, 895, pp. 96-101. 2019. <https://doi.org/10.4028/www.scientific.net/AMM.895.96>
- 22 Czichos, H., Becker, S., and Lexow, J., *Wear*, Vol 114, pp 109-130. 1987. [https://doi.org/10.1016/0043-1648\(87\)90020-2](https://doi.org/10.1016/0043-1648(87)90020-2)
- 23 Manual on Quality Control of Materials, ASTM STP 15D, ASTM, 1951.
24. Singh, G. and Goyal, S. Microstructure and mechanical behavior of AA6082-T6/SiC/B4C-based aluminum hybrid composites. *Particulate Science and Technology*, 36(2), pp.154-161. 2014. <https://doi.org/10.1080/02726351.2016.1227410>
- 25 ASTM Standards 2
26. Y.Q. Wang, J.I. Song "Temperature effects on the dry sliding wear of Al₂O₃f/SiCp/Al MMCs with different fiber orientations and hybrid ratios", Elsevier-Wear, Volume 270, Issues 7-8, Pages 499-505, 10. 2011. <https://doi.org/10.1016/j.wear.2011.01.002>
27. Abdizadeh, H. and Baharvandi, H.R. Development of high-performance A356/nano-Al₂O₃ composites *Mater. Sci. Eng. A*, 518, pp.61-64. 2009. <https://doi.org/10.1016/j.msea.2009.04.014>
- 28 Kaibyshev, R., Sitdikov, O., Mazurina, I. and Lesuer, D.R. Deformation behavior of a 2219 Al alloy. *Materials Science and Engineering: A*, 334(1-2), pp.104-113. 2002. [https://doi.org/10.1016/S0921-5093\(01\)01777-4](https://doi.org/10.1016/S0921-5093(01)01777-4)
- 29 Biswas, S., Dwarakadasa, E. and Biswas, S. K. "Bearings and wear properties of cast graphite aluminium composites", *Proceedings of All India Seminar on Aluminium*, pp 189-196. 1979.
- 30 G. Straffelini, M. Pellizzari, A. Molinari "Influence of load and temperature on the dry sliding behaviour of Al-based metal-matrix-composites against friction

- material", Elsevier-Wear, Volume 256, Issues 7-8, Pages 754-763, 2004. [https://doi.org/10.1016/S0043-1648\(03\)00529-5](https://doi.org/10.1016/S0043-1648(03)00529-5)
- 31 Heguo Zhu a,n, CuicuiJar a, JinzhuSong a, JunZhao a, JianliangLi a, ZonghanXie b,nn "Microstructure and high temperature wear of the aluminium matrix composites fabricated by reaction technique from Al-ZrO₂-B elemental powder", Elsevier-Powder Technology, Volume 217, Pages 401-408. 2012. <https://doi.org/10.1016/j.powtec.2011.10.056>
- 32 Heguo Zhu a, n, CuicuiJar a, JinzhuSong a, JunZhao a, JianliangLi a, ZonghanXie b, nn "High temperature dry sliding friction and wear characteristics of in situ composites (a-Al₂O₃βAl₃Zr)/Al", Advanced Materials Research, Vols. 690-693, pp. 318-322, 2013. <https://doi.org/10.4028/www.scientific.net/AMR.690-693.318>
- 33 Hassan, A.M., Alrashdan, A., Hayajneh, M.T. and Mayyas, A.T. Prediction of density, porosity and hardness in aluminum-copper-based composite materials using artificial neural network. Journal of materials processing technology, 209(2), pp.894-899. 2009. <https://doi.org/10.1016/j.jmatprotec.2008.02.066>
- 34 Zhang, Z., Barkoula, N.M., Karger-Kocsis, J. and Friedrich, K. Artificial neural network predictions on erosive wear of polymers. Wear, 255(1-6), pp.708-713. 2003. [https://doi.org/10.1016/S0043-1648\(03\)00149-2](https://doi.org/10.1016/S0043-1648(03)00149-2)
- 35 Jiang, Z., Zhang, Z. and Friedrich, K. Prediction on wear properties of polymer composites with artificial neural networks. Composites Science and Technology, 67(2), pp.168-176. 2007. <https://doi.org/10.1016/j.compscitech.2006.07.026>